Supplementary Material

Table S1: ^{14}C-AMS dates in cores GeoB3938-1 and GeoB7010-2

				Radiocarbon age		**Calendar age**[1]	
Core	Sample	Species	Depth (cm)	Mean (a BP)	1 std dev (a BP)	Mean (a BP)	1 std dev (a BP)
GeoB3938-1	Beta Analytic 348091	*G. ruber*	5	4250	30	4340	55
	Beta Analytic 348092	*G. ruber*	20	9750	50	10600	60
	Beta Analytic 348093	*G. ruber*	66	21630	90	25400	200
	Beta Analytic 348094	*G. ruber*	95	26250	140	30700	175
GeoB7010-2	Poz-46048	*G. sacculifer*	42	6570	40	7100	60
	Poz-46049	*G. sacculifer*	86	10850	60	12340	110
	Poz-46050	*G. sacculifer*	126	15020	80	17790	145
	Poz-46051	*G. sacculifer*	134	16230	100	18930	100
	Poz-46052	*G. sacculifer*	190	24330	210	28780	310
	Poz-46053	*G. sacculifer*	250	32320	520	26550	400
	Poz-46054	*G. sacculifer*	345	43500	2000	46600	1750

[1] ^{14}C ages were converted into calendar ages using the CALIB radiocarbon calibration software (version 6.1.0, http://calib.qub.ac.uk/calib/) and the Marine09 calibration curve (reservoir age of 400 a).

Table S2: Characteristic elemental proportions and log-ratios of river suspended material. Mean and 1 standard deviation were calculated from values given in Table S3.

Rivers	Al (%)	Si (%)	K (%)	Ca (%)	Ti (%)	Fe (%)	ln(Al/Si)	ln(Fe/K)	ln(Al/K)
Orinoco River	21.3 ± 2.5	63.1 ± 2.8	3.0 ± 0.8	0.9 ± 0.2	1.5 ± 0.3	10.2 ± 1.5	-1.09 ± 0.16	1.25 ± 0.39	1.99 ± 0.37
Amazon River	23.9 ± 0.5	55.8 ± 1.3	5.1 ± 0.7	1.8 ± 0.8	1.2 ± 0.2	12.3 ± 1.1	-0.85 ± 0.05	0.89 ± 0.12	1.56 ± 0.05
Amazon Andean tributaries	21.8 ± 1.5	59.3 ± 2.7	5.2 ± 0.6	1.2 ± 0.7	1.2 ± 0.1	11.3 ± 1.1	-1.00 ± 0.12	0.79 ± 0.17	1.45 ± 0.15
Amazon lowland tributaries	34.4 ± 2.9	45.0 ± 0.0[1]	2.0 ± 1.8	1.1 ± 0.7	1.3 ± 0.2	16.2 ± 2.4	-0.27 ± 0.08	2.13 ± 0.74	2.92 ± 0.75

[1] See footnote 3 in Table S3.

Table S3: Major element composition of river suspended material used in the endmember unmixing analysis. (Elemental proportions are given in weight percent and were calculated such as the sum of the six elements considered in this study is 100 %.)

	River	Lat	Long	Al (%)	Si (%)	K (%)	Ca (%)	Ti (%)	Fe (%)	Reference
1	Orinoco	9.1[1]	-61.6[1]	23.3	60.2	2.2	0.7	1.7	12.0	Martin & Meybeck (1979)
2	Orinoco	9.1[1]	-61.6[1]	18.6	65.8	3.7	1.2	1.2	9.6	McLennan (1993); Hirst (1962)
3	Orinoco	9.1[1]	-61.6[1]	22.1	63.2	2.9	0.8	1.8	9.1	Eisma et al. (1978)
4	Amazon	-1.2[1]	-51.7[1]	24.1	55.9	3.8	3.3	1.5	11.5	Martin & Meybeck (1979)
5	Amazon	-1.2[1]	-51.7[1]	24.5	53.5	5.0	1.5	0.9	14.5	Sholkovitz et al. (1978)
6	Amazon (AM-06-59)	-1.9	-55.5	22.9	57.5	5.3	1.5	1.2	11.6	Bouchez et al. (2011)
7	Amazon (AM-06-62)	-1.9	-55.5	24.0	55.8	5.4	1.4	1.2	12.2	Bouchez et al. (2011)
8	Amazon (AM-06-65)	-1.9	-55.5	23.8	56.2	5.4	1.4	1.2	12.1	Bouchez et al. (2011)
9	Amazon (AM-06-52)	-2.6	-55.6	23.9	55.7	5.6	1.4	1.2	12.3	Bouchez et al. (2011)
10	Madeira (AM-06-35)	-3.4	-58.8	22.8	57.7	5.9	0.7	1.2	11.8	Bouchez et al. (2011)
11	Madeira (AM-06-38)	-3.4	-58.8	19.4	63.4	5.2	0.7	1.2	10.2	Bouchez et al. (2011)
12	Madeira (AM-06-41)	-3.4	-58.8	20.5	61.4	5.6	0.7	1.2	10.5	Bouchez et al. (2011)
13	Madeira (AM-06-43)	-3.4	-58.8	21.5	60.1	5.6	0.6	1.2	10.9	Bouchez et al. (2011)
14	Solimões (AM-06-09)	-3.3	-60.5	22.0	59.2	4.6	1.9	1.1	11.1	Bouchez et al. (2011)
15	Solimões	-3.3	-60.5	22.5	58.4	4.7	2.0	1.1	11.2	Bouchez et al. (2011)

	(AM-06-14)									
16	Solimões (AM-06-19)	-3.3	-60.5	24.1	55.0	4.5	2.0	1.1	13.5	Bouchez et al. (2011)
17	Negro[2] (MAO 01)	-3.1	-60.3	38.2	45[3]	1.3	0.5	1.5	13.5	*this study*
18	Negro[2] (MAO 02f)	-3.1	-60.3	30.6	45[3]	5.7	2.5	1.4	14.8	*this study*
19	Negro[2] (MAO 03c)	-3.1	-60.2	38.3	45[3]	1.7	0.5	1.4	13.2	*this study*
20	Negro[2] (MAO 81)	-3.0	-60.4	32.4	45[3]	2.5	1.3	1.5	17.3	*this study*
21	Negro[2] (MAO 83)	-3.1	-60.3	33.4	45[3]	0.7	1.0	1.4	18.4	*this study*
22	Negro[2] (MAO 93)	-3.2	-60.0	33.5	45[3]	0.0	0.8	1.4	19.2	*this study*
23	Negro	-2.0[1]	-61.2[1]	34.6	45.0	1.8	0.9	0.8	17.0	Sholkovitz et al. (1978)

[1] Approximate latitude and longitude

[2] The sampling of suspended material was carried out during periods of low (November 2011) and high (May 2012) river flow. For each period, we collected water from three sites using a submersible pump at 60 % of the water depth in the deepest portion of the Negro river channel. At least 4 litres of water was filtered using cellulose filters (0.2 µm), which were immediately dried and packed in plastic bags for transportation. Digestion of suspended material was carried out with a microwave system (MLS, 1200 MEGA). For this purpose, 7 ml HNO_3 (65%), 0.5 ml HF (40%), 0.5 ml HCl (30%), and 0.5 ml MilliQ were added to about 21-89 mg sample material (filter + suspended material) previously placed into Teflon liners. All acids were of suprapure quality. Element concentrations were measured with ICP-OES (Agilent 720; precision: 2 %, standard deviation: 1-3 %).

[3] Because of Si loss during total digestion procedure, the Si proportion of new Negro samples is fixed to 45 %, based on available data from Sholkovitz et al. (1978). An error of ± 2.5 % on Si proportion is included in the endmember unmixing analysis. We run three sets of 1000 Monte-Carlo iterations with different Si proportions of Negro samples (45 %, 42.5 % and 47.5 %).

Table S4: Summary of the terrigenous and marine biogenic endmembers (EM) used in the unmixing analysis (Methods section 3.4) for the three cores. Numbers in terrigenous EM columns refer to Supplementary Table 3.

Lat	Core	1st terrigenous EM	2nd terrigenous EM	Marine EM[1]
12°N	GeoB3938-1	Amazon	Orinoco	98 (± 1) % Ca
		(4-9)	(1-3)	2 (± 1) % Si
9°N	GeoB7010-2	Amazon lowland tributaries	Amazon Andean tributaries	98 (± 1) % Ca
	GeoB7011-1	(17-23)	(10-16)	2 (± 1) % Si
5°N	GeoB4411-2	Amazon lowland tributaries	Amazon Andean tributaries	98 (± 1) % Ca
		(17-23)	(10-16)	2 (± 1) % Si

[1] The marine biogenic endmember is composed of Ca and Si only. Its composition is derived from the carbonate and biogenic opal content of surface sediment in nearby sites (data from Lochte et al. (2000), available here: http://doi.pangaea.de/10.1594/PANGAEA.53229). Values in brackets are the errors on the composition that are included in the 95% confidence intervals of the endmember unmixing analysis.

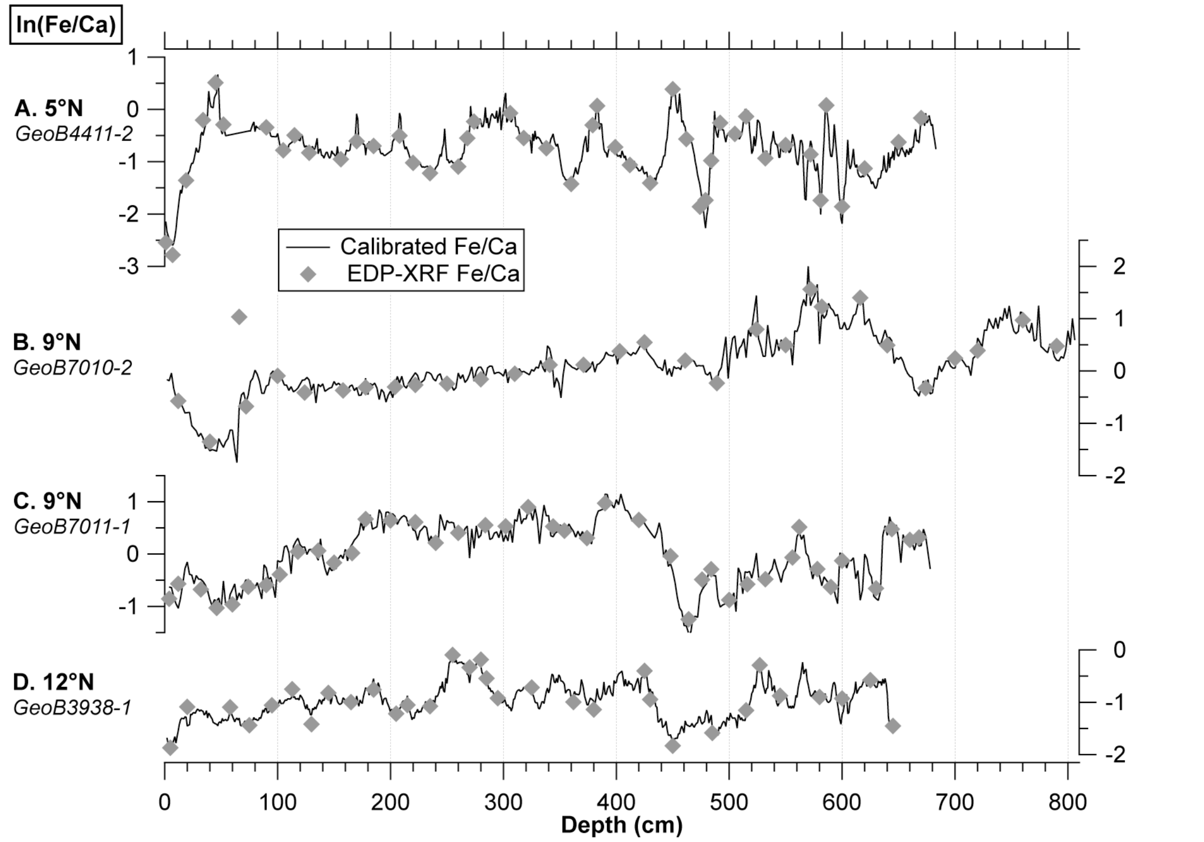

Fig. S1: Quality of XRF calibration. Downcore ln(Fe/Ca) variations obtained from calibrated major element proportions (black line) and EDP-XRF measurements (grey diamonds) are presented versus depth for cores: A. GeoB4411-2 (r^2=0.96), B. GeoB7010-2 (r^2=0.91), C. GeoB7011-1 (r^2=0.94) and D. GeoB3938-1 (r^2=0.85). The given r^2 value is the mean r^2 of all element/Ca log-ratio regressions (Weltje and Tjallingii, 2008).

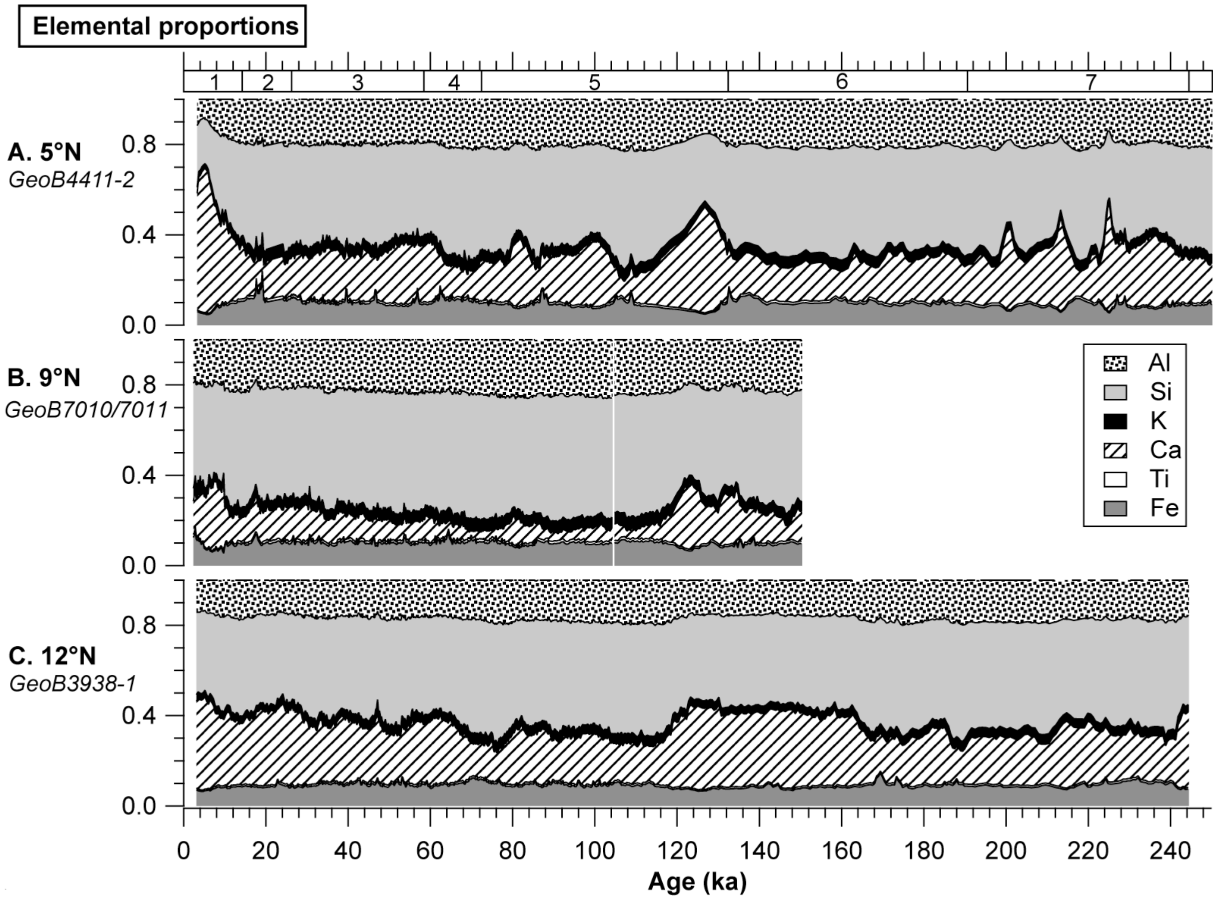

Fig. S2: Variations in major element calibrated proportions (Al: dots; Si, light grey area; K, black area; Ca: hatched area; Ti: white area; Fe, medium grey area) from sites at A. 5°N: GeoB4411-2, B. 9°N: GeoB7010-2 (0-104 ka) and GeoB7011-1 (105-150 ka) and C. 12°N: GeoB3938-1. Elemental proportions vary between 0 (0 %) and 1 (100 %). Ti proportions (white area) are very low (< 2 %) and hardly distinguishable between the Fe and Ca proportions. Marine Isotope Stages are indicated at the top of A.

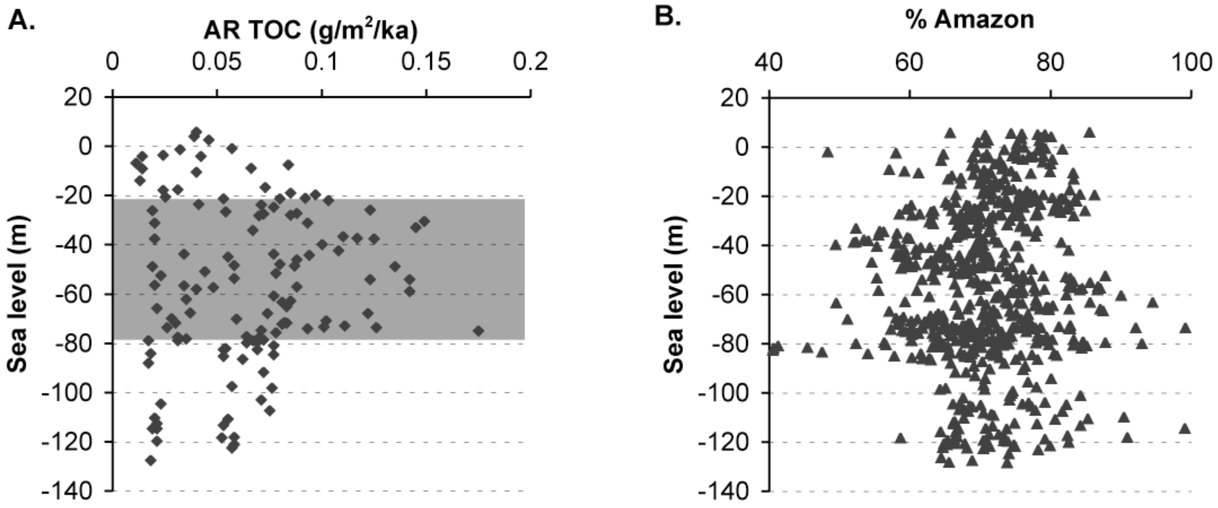

Fig. S3: A. Accumulation rate (AR) of the total organic carbon (TOC) (Schlünz et al., 2000) and B. %-Amazon (this study) from core GeoB3938-1 (12°N) plotted against sea level (data from Waelbroeck et al., 2002). The grey rectangle (in A) highlights the phase of intermediate sea levels where the TOC might be enhanced according to Schlünz et al. (2000). We do not observe any relationship between sea level and %-Amazon in this core.

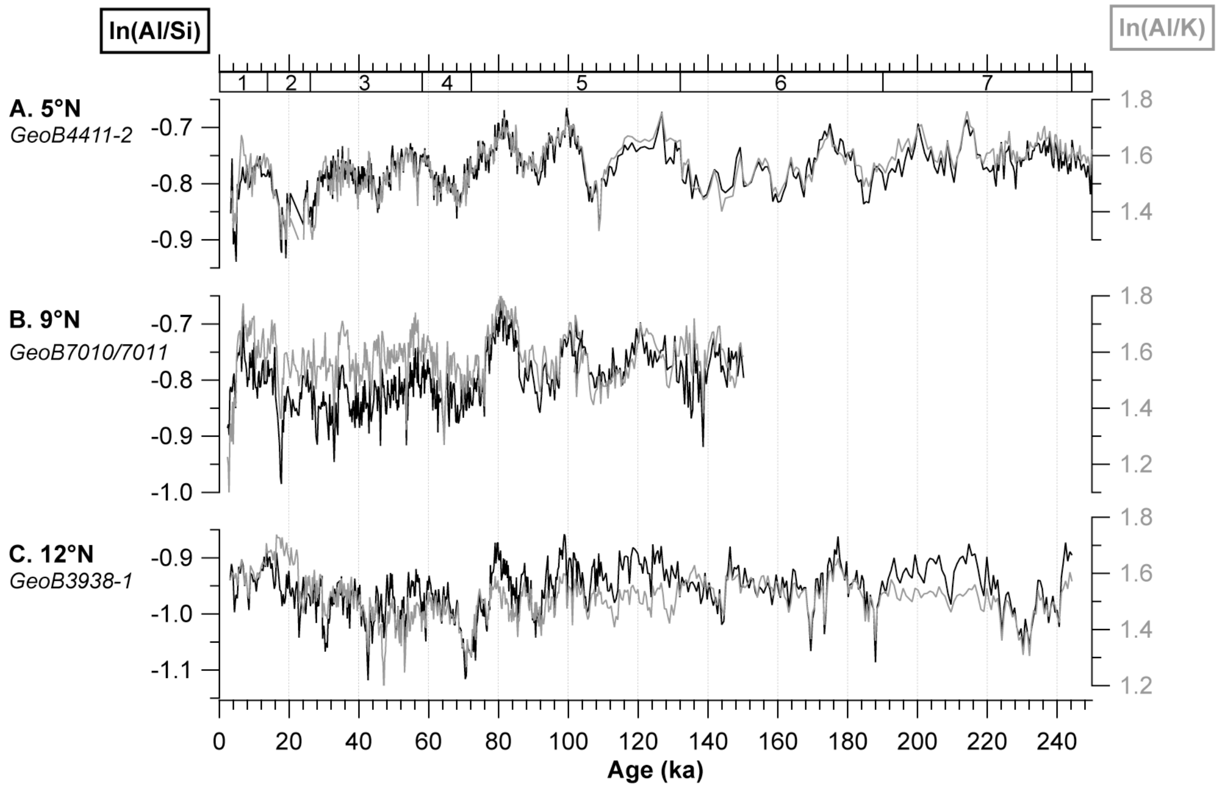

Fig. S4: Al/Si (left ordinate axis, black curve) and Al/K (right ordinate axis, grey curve) log-ratios from cores A. 5°N: GeoB4411-2, B. 9°N: GeoB7010-2 (0-104 ka) and GeoB7011-1 (102-150 ka), and C. 12°N: GeoB3938-1. Marine Isotope Stages are indicated at the top of A.

References in Supplementary Material

Bouchez, J., Gaillardet, J., France-Lanord, C., Maurice, L., and Dutra-Maia, P.: Grain size control of river suspended sediment geochemistry: Clues from Amazon River depth profiles, Geochem. Geophys. Geosyst., 12, Q03008, 10.1029/2010gc003380, 2011.

Eisma, D., Van Der Gaast, S. J., Martin, J. M., and Thomas, A. J.: Suspended matter and bottom deposits of the Orinoco delta: Turbidity, mineralogy and elementary composition, Netherlands Journal of Sea Research, 12, 224-251, 10.1016/0077-7579(78)90007-8, 1978.

Hirst, D. M.: The geochemistry of modern sediments from the Gulf of Paria--I The relationship between the mineralogy and the distribution of major elements, Geochimica et Cosmochimica Acta, 26, 309-334, 10.1016/0016-7037(62)90017-0, 1962.

Lochte, K., Boetius, A., Gebruk, A., Helder, W., Jahnke, R. A., Pfannkuche, O., Rabouille, C., Schlüter, M., Shimmield, G., Sibuet, M., Soltwedel, T., Vetrov, A. A., and Zabel, M.: Atlantic data base for exchange processes at the deep sea floor (ADEPD). Data collected and published through EU-project ADEPD (MAS3-CT97-0126-ADEPD) 1998/99, Institute for Baltic Sea Research, Warnemünde, Germany, 2000.

Martin, J.-M., and Meybeck, M.: Elemental mass-balance of material carried by major world rivers, Marine Chemistry, 7, 173-206, 10.1016/0304-4203(79)90039-2, 1979.

McLennan, S. M.: Weathering and Global Denudation, The Journal of Geology, 101, 295-303, 10.1086/648222, 1993.

Schlünz, B., Schneider, R. R., Müller, P. J., and Wefer, G.: Late Quaternary organic carbon accumulation south of Barbados: influence of the Orinoco and Amazon rivers?, Deep Sea Research Part I: Oceanographic Research Papers, 47, 1101-1124, 10.1016/S0967-0637(99)00076-X, 2000.

Sholkovitz, E. R., van Grieken, R., and Eisma, D.: The major-element composition of suspended matter in the Zaire river and estuary, Netherlands Journal of Sea Research, 12, 407-413, 10.1016/0077-7579(78)90042-X, 1978.

Waelbroeck, C., Labeyrie, L., Michel, E., Duplessy, J. C., McManus, J. F., Lambeck, K., Balbon, E., and Labracherie, M.: Sea-level and deep water temperature changes derived from benthic foraminifera isotopic records, Quaternary Science Reviews, 21, 295-305, 2002.

Weltje, G. J., and Tjallingii, R.: Calibration of XRF core scanners for quantitative geochemical logging of sediment cores: Theory and application, Earth and Planetary Science Letters, 274, 423-438, 10.1016/j.epsl.2008.07.054, 2008.